Two Methods for Correcting Range-Dependent Limitations of Lightning Mapping Arrays

STEPHANIE A. WEISS[a]

Cooperative Institute for Mesoscale Meteorological Studies, University of Oklahoma, and NOAA/National Severe Storms Laboratory, Norman, Oklahoma

DONALD R. MACGORMAN

NOAA/National Severe Storms Laboratory, Norman, Oklahoma

ERIC C. BRUNING

Texas Tech University, Lubbock, Texas

VANNA C. CHMIELEWSKI

NOAA/National Severe Storms Laboratory, Norman, Oklahoma

(Manuscript received 11 December 2017, in final form 14 April 2018)

ABSTRACT

Lightning Mapping Arrays (LMAs) detect very high frequency (VHF) radiation produced by lightning as it propagates; however, VHF source detection efficiency drops off rapidly with range from the centers of the arrays, which results in a maximum of source points over the center of the network for large datasets. Using data from nearly one billion detected sources of various powers, an approximation of VHF source detection efficiency (relative to the number of sources detected within 25 km of the center of the array) for the Oklahoma LMA is calculated for different ranges and source powers. The calculated source detection efficiencies are then used to normalize the VHF source data out to a range of 125 km, as a method for correcting the detection efficiency drop-off with range. The data are also sorted into flashes using a popular flash-sorting algorithm in order to compare how well flash sorting corrects for detection efficiency drop-off with range compared to the normalization method. Both methods produce similar patterns and maxima of the lightning location, but the differences between them are identified and highlighted. The use of a flash-sorting algorithm is recommended for future studies involving large sets of data.

1. Introduction

The Oklahoma Lightning Mapping Array (OKLMA) has collected the time and location of very high frequency (VHF) radiation sources produced by all types of lightning in central Oklahoma since the spring of 2003 (MacGorman et al. 2008). As one of the longest-running Lightning Mapping Arrays (LMAs) in the country (Rison et al. 1999), there is a unique opportunity to combine the data into a single dataset that can be mined for useful long-term information on the climate and impact of thunderstorms in central Oklahoma. One of the limitations of using the LMA for climatological applications is that it is a local system, generally limited to a radius of 200 km (Thomas et al. 2004), and its source detection efficiency varies with time and is range dependent, with the greatest detection efficiency directly over the network. For investigating local storms and flashes, this limitation has minimal adverse impacts; but when looking at an entire season of thunderstorms, the disproportionately large number of sources detected directly above the array gives a false sense of where there are maxima in lightning activity.

Denotes content that is immediately available upon publication as open access.

[a] Current affiliation: Texas Tech University, Lubbock, Texas.

Corresponding author: Stephanie A. Weiss, stephanie.weiss@ttu.edu

DOI: 10.1175/JTECH-D-17-0213.1

One way of trying to overcome the problem of greater efficiency of the LMA close to the network is to sort the VHF sources into flashes and to consider the number of flashes that propagate over a location rather than the number of sources detected over a location. Using this method assumes that the flash detection efficiency is not dependent on range from the network's center, which is not necessarily the case. Supercell thunderstorms, in particular, are known to have a large quantity of very small flashes that could easily be missed at greater ranges from the network (e.g., Kuhlman et al. 2006; Bruning and MacGorman 2013). Trends in flash rates are used operationally to help detect thunderstorm intensification (e.g., Schultz et al. 2009; Darden et al. 2010; Chronis et al. 2015), so it is important to understand whether this method reliably eliminates detection efficiency discrepancies across the network.

With the operational implications in mind and with the goal of being able to develop a lightning climatology for central Oklahoma, a second method for correcting for the range effects of the LMA is presented. This second method normalizes the number of VHF sources at different ranges using source detection efficiencies calculated relative to the number of sources detected at the center of the network and assuming that the fraction of VHF sources detected at various ranges across the network is stable. The normalized number of VHF sources is converted to a proxy for flashes (the number of seconds with at least one VHF source, or lightning-seconds) and is then compared to the lightning flash extent densities over the same region and time period to see how well the flash-sorting method does at mitigating the range effect problem.

2. LMA accuracy and detection efficiency

Lightning Mapping Arrays locate the sources of VHF radiation emitted by lightning propagation in three spatial dimensions and in time. The accuracy of the locations depends on uncertainty in the arrival time measurements and on the number and positions of stations that detect the radiation (e.g., Koshak et al. 2004; Thomas et al. 2004). Thomas et al. (2004) found that sources over the network are located with a root-mean-square uncertainty of 6–12 m in the horizontal, 20–30 m in the vertical, and 40–50 ns in time. They also found that the range and altitude errors increase as the range squared and that azimuthal error increases linearly with range, causing lightning in storms to appear spread radially when plotted in a plan view (e.g., Fig. 15 in Thomas et al. 2004).

The location accuracy of the LMA has been well documented, but its detection efficiency is harder to determine and is dependent on the number of stations in operation, the configuration of the array, and the signal threshold of each station (e.g., Chmielewski and Bruning 2016). Hamlin (2004) investigated the minimum detectable signal needed for detection at different ranges from the network, both for simulated source locations and for case studies of sparks emitted by airplanes as they flew through cirrus clouds. He showed that the source power is proportional to the square of the distance between the source and the receiving antenna:

$$P_s = P_r \times \frac{(4\pi r)^2}{G\lambda^2}, \tag{1}$$

where P_s is the source power, P_r is the received power, r is the distance between the source and the receiving antenna, G is the antenna gain, and λ is the wavelength. In other words, the required source power for detection is parabolic and asymptotically bound by the square of the distance between the source and the receiving antenna.

Two more ways of seeing the difference in detection of source power with range are shown in Fig. 1. The plots in Fig. 1 contain reprocessed data from five of the most lightning-intense months in terms of both spatial coverage and flash density in the OKLMA dataset (June 2007, 2008, 2009, 2010, and 2011), a total of nearly one billion (991 414 533) VHF source points. For these plots (and for all data used in this study), a χ^2 value < 1 [based on a 70-ns timing error, as in Thomas et al. (2004)] and detection by at least six stations are required for a VHF source to be included, and only sources at an altitude between 0 and 20 km and within 200 km of the network's center are used. The plots in Fig. 1 show how the detectability of low-power sources drops off with distance from the network. The minimum source powers detected increase with distance from the center of the network in the parabolic relationship predicted by Hamlin (2004).

a. Source detection efficiency

The ability of LMAs to detect VHF sources depends on many factors, such as the number and configuration of stations in operation at any given time and the individual receiver thresholds, which make it difficult to calculate a definitive source detection efficiency for a network. However, an approximation of source detection efficiency relative to the center of the LMA, where detection is optimal, can be calculated by assuming a source detection efficiency of 100% directly over the network and then computing the ratio of the number of sources per area detected at each annulus (25–50, 50–75 km, etc.) to the number of sources per area detected within 25 km of the center of the LMA for each detected source power. These calculations were done for the OKLMA using the data from the plots in

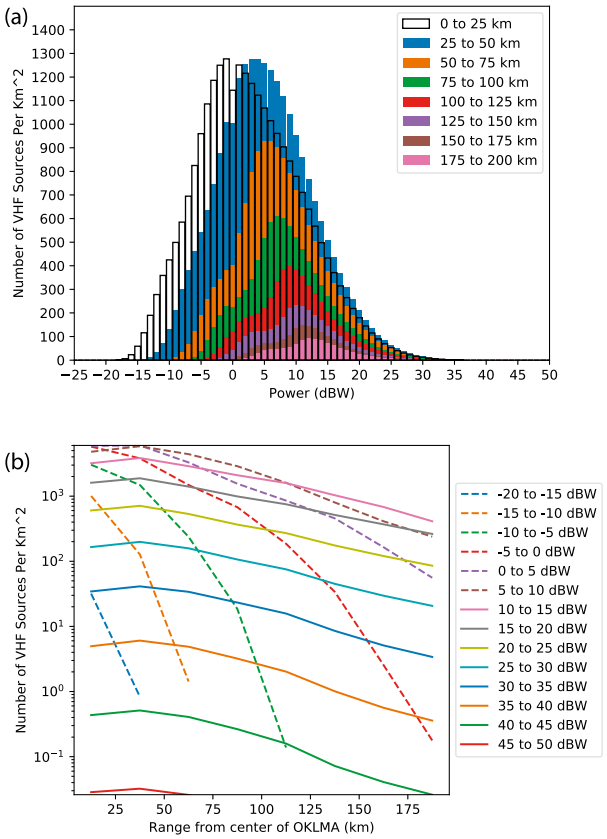

FIG. 1. (a) Density of LMA sources (with each power value in dBW) for different ranges from the center of the LMA is given for June for five years — 2007–11. As expected, there is a significant drop-off in detectable power with distance from the center of the LMA. The 125–150-km-range annulus was chosen as the basis for normalization, such that all sources within 125 km of the center of the array were run through a filter that made each power spectra match that of the one for the 125–150-km-range annulus. (b) Same data as in (a), but plotted as density changing with range from the center of the LMA for different VHF source powers.

Fig. 1, and the results are shown in the numbers in parentheses in Table 1. It is understood that the dataset used for these calculations is a real-world dataset that does not have a uniform number of VHF sources across the different ranges, that the source detection efficiency directly over the network is not actually 100%, and that the source detection efficiency will change over time with receiver sensitivity and noise. The source detection efficiencies presented here are not meant to be the definitive source detection efficiencies for the OKLMA; rather, they are included as a reference for future studies of what an operational instrument in real-world conditions can achieve.

The source detection efficiencies observed here drop off more quickly with range than those calculated by Chmielewski and Bruning (2016) using a Monte Carlo simulation. For example, the simulated detection efficiencies are 99%/88%/70% at 100/150/200 km, respectively (Fig. 6h in Chmielewski and Bruning 2016), whereas the weighted averages of the observed source detection efficiencies found in Table 1 are 48%, 24%, and 14% at 75–100, 125–150, and 175–200 km, respectively. One reason the simulated source detection efficiencies are higher than the observed source detection efficiencies is that Chmielewski and Bruning (2016) used constant receiver threshold values and an idealized source power distribution based on observations in New Mexico in their original computation.

b. *Flash detection efficiency*

The simulation by Chmielewski and Bruning (2016) originally estimated the flash detection efficiency to be greater than 95% out to 200 km from the center of the OKLMA network; however, calculations of flash detection efficiency are dependent on source detection efficiency. Given a source detection efficiency of x, a minimum 10-point flash can be resolved if the flash, perfectly detected, would have contained at least $10/x$ points. The flash detection efficiency is then estimated as the percentage of well-resolved flashes with at least $10/x$ points from the climatology presented in Chmielewski and Bruning (2016). Using the newly calculated and simulated source detection efficiencies, new flash detection efficiencies were computed to be 91%, 79%, and 70% at 100, 150, and 200 km, respectively. The fact that Chmielewski and Bruning (2016) used constant receiver thresholds and an idealized source power distribution for their original source detection efficiency calculations also accounts for the higher flash detection efficiencies. Running the simulation again using receiver threshold values 8–10 dBW higher yielded flash detection efficiencies matching those computed using the power spectrum from the observed data (Fig. 2). For consistency between this study and those previously published, these newly calculated flash detection efficiencies are not accounted for in the flash-sorting method detailed in this manuscript.

As noted earlier, trends in flash rates are used operationally to detect thunderstorm intensification (e.g., Schultz et al. 2009; Darden et al. 2010; Chronis et al. 2015), often using a statistically significant increase in lightning activity over a short period known as a lightning jump (LJ) as an indicator of storm intensification. It is important to consider whether an increase in flash detection efficiency as a storm moves toward the center of an LMA in and of itself accounts for enough of an increase in flash rate to change the outcome of these LJ algorithms. Assuming a constant flash rate of 100 flashes per minute in a storm moving from west to east across an

TABLE 1. A normalization method was used to remove VHF sources from the original dataset to offset the change in source detection efficiency with range from the center of the LMA. This table contains percentages of sources removed for different ranges and source powers, which were calculated using Eq. (2). The values in parentheses are the approximations of source detection efficiencies for the OKLMA for each source power and range annulus, which are calculated using five months of data (Junes 2007–11) and with the assumption that the detection efficiency is 100% within 25 km from the center of the OKLMA.

	Power (dBW)											
Range (km)	−4	0	5	10	15	20	25	30	35	40	45	50
0–25	100 (100)	96 (100)	88 (100)	70 (100)	66 (100)	71 (100)	72 (100)	74 (100)	78 (100)	83 (100)	82 (100)	36 (100)
25–50	100 (58)	96 (88)	90 (100)	75 (100)	71 (100)	75 (100)	77 (100)	79 (100)	82 (100)	86 (100)	83 (100)	65 (100)
50–75	100 (24)	89 (35)	87 (87)	67 (93)	62 (87)	66 (87)	70 (93)	74 (99)	78 (100)	83 (96)	76 (75)	68 (100)
75–100	100 (8)	81 (20)	76 (48)	55 (67)	46 (62)	51 (60)	56 (63)	62 (67)	67 (67)	73 (62)	59 (44)	32 (95)
100–125	97 (1)	66 (11)	44 (21)	39 (49)	31 (48)	35 (45)	38 (45)	45 (46)	50 (43)	55 (37)	56 (40)	48 (100)
125–150	0 (0)	0 (4)	0 (12)	0 (30)	0 (34)	0 (29)	0 (28)	0 (26)	0 (22)	0 (17)	0 (18)	0 (64)
150–175	0 (0)	0 (0)	0 (7)	0 (17)	0 (24)	0 (21)	0 (19)	0 (16)	0 (13)	0 (9)	0 (16)	0 (52)
175–200	0 (0)	0 (0)	0 (4)	0 (8)	0 (17)	0 (15)	0 (13)	0 (11)	0 (8)	0 (6)	0 (12)	0 (60)

LMA network, the computed flash detection efficiencies given above indicate that the network would detect an increase of 12 flashes as the storm moved from 150 km west of the center of the array to 100 km west of the center of the array. Even if the storm is moving at a relatively fast speed—that is, 26.5 m s^{-1}—the flash rate of the storm would increase only by 0.38 flashes per minute over that distance. The change in flash rate of a storm moving across an LMA network caused by the change in flash detection efficiency across that network is not enough in and of itself to affect the LJ algorithms used in operational settings.

3. Correction methods

Two methods for correcting for the limitations in detection of low-power VHF sources over the network were investigated: a normalization method and the flash-sorting method. For both methods, the data were aggregated in 10 km × 10 km grid cells. Each method is applied to the nearly one billion VHF sources found in Fig. 3a—the combination of all VHF sources meeting the previously stated criteria from June 2007, June 2008, June 2009, June 2010, and June 2011. For the normalization method, the density of lightning-seconds was analyzed as a way for emulating flashes, which makes for a better direct comparison to the flash densities that were calculated by the flash-sorting method.

a. Normalization method

For the normalization method, a percentage of VHF sources within 125 km of the center of the network were removed from the dataset to normalize the data across the network, with the percentage of sources removed being dependent on distance from the center of the network. To do this, the data first were divided into groups every 25 km from the center of the network. The sources detected in the 125–150-km annulus were then used to normalize the data. This annulus was chosen because it is the range at which there is the steepest decline in detection efficiency and where the source detection efficiency reaches approximately 25% (see section 2a). The number of sources removed from each group was determined by the emitted power of the individual VHF sources and based on the power spectra shown in Fig. 1a. Which sources were removed was determined with a random draw. For each P_s from $P_s = -4$ to 50 dBW, the percentage of sources removed for each range was

$$100 - \left[\left(\frac{n_{125}A_n}{nA_{125}}\right) \times 100\right], \tag{2}$$

where n_{125} is the number of sources in the 125–150-km annulus, n is the number of sources in the annulus

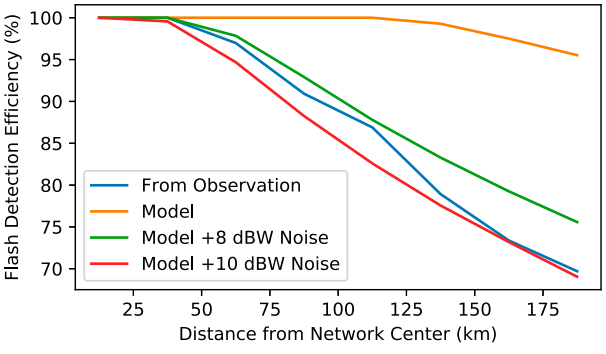

FIG. 2. Flash detection efficiencies with range from the center of the OKLMA computed using the method outlined in Chmielewski and Bruning (2016). The flash detection efficiencies calculated using the observed data from the power spectra shown in Fig. 1a (blue line) are lower than those calculated in the original model (orange line), which used constant receiver threshold values and an idealized power spectra. The observed flash detection efficiencies can be recreated with the model by increasing the receiver threshold values by between 8 (green line) and 10 dBW (red line).

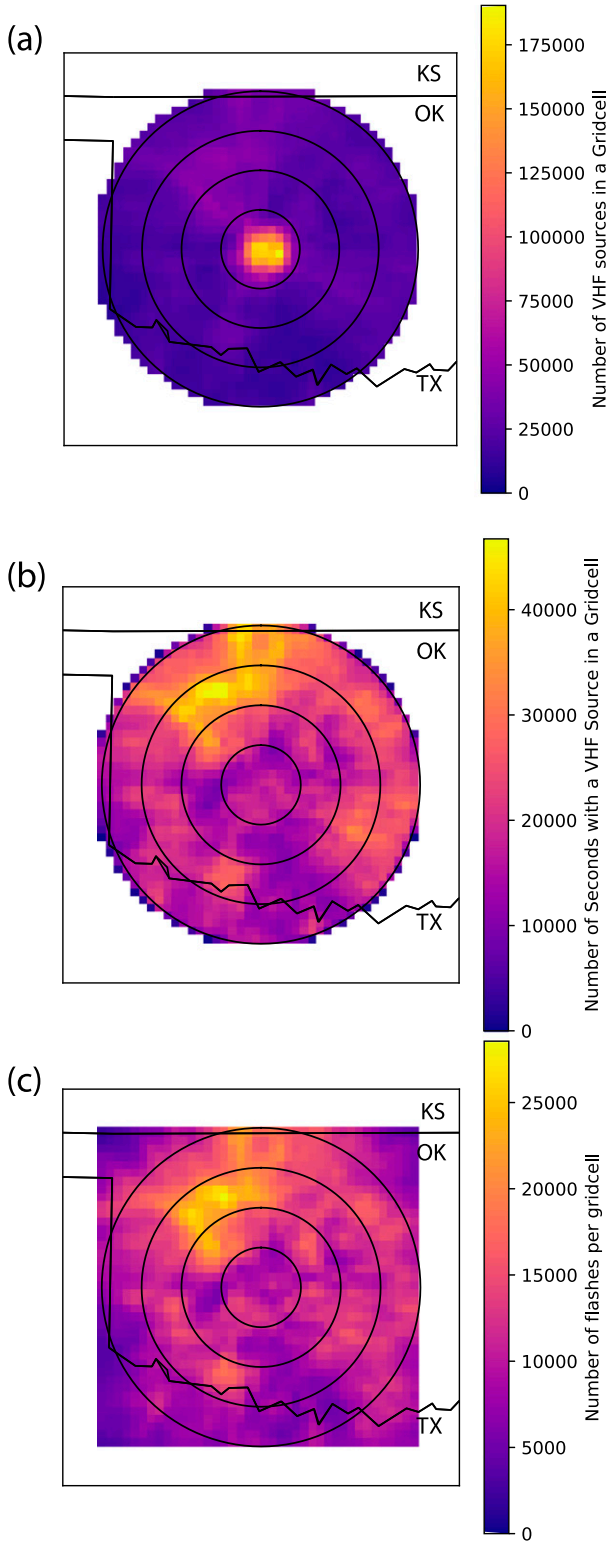

FIG. 3. (a) All VHF sources detected by the OKLMA from June 2007, June 2008, June 2009, June 2010, and June 2011 that were within 200 km of the center of the OKLMA, were below 20 km in altitude, had a χ^2 value < 1, and were detected by at least six stations are shown for each 10 km $\times$ 10 km cell. The colors indicate the number of VHF sources detected in each grid cell, with warm-colored grid cells containing more sources. The black rings are plotted every 50 km from the center of the LMA network. (b) The density of lightning-seconds for the same period as (a), after the data have been normalized to the 125–150-km range annulus using power values based on the power spectra shown in Fig. 1a. (c) As in (a), except the colors represent flash extent densities instead of individual LMA sources.

(or circle) being normalized, A_n is the area of the annulus (or circle) being normalized, and A_{125} is the area of the 125–150-km annulus. Beyond 125 km no adjustment is made. (Note that normalizing at a range beyond 125 km is possible but a larger range of signal amplitudes would be removed.) The results of this calculation for each power at each range are shown in Table 1. The values in Table 1 are assumed to be representative of the overall performance of the OKLMA from 2007 to 2011 and are used for the normalization of all the datasets presented in this manuscript. After the appropriate percentage of VHF sources are randomly removed from a dataset, the number of seconds with at least one VHF source (lightning-seconds) is calculated for each grid cell. Isolated VHF sources are not removed by this method, but a comparison between the number of lightning-seconds recorded on days with no thunderstorms (all noise) and the number recorded on days with thunderstorms determined that the percentage of lightning-seconds caused by noise is negligible (i.e., 0.066% for a day with a large-scale lightning event and 0.18% for a day with a small-scale lightning event). The result of using the normalization method on the data from Junes in 2007–11 is shown in Fig. 3b.

b. *Flash-sorting method*

For the flash-sorting method, flashes were sorted using the method developed by McCaul et al. (2009), and all flashes with fewer than 10 sources were discarded. With the McCaul et al. (2009) method of flash sorting, individual VHF sources are grouped into flashes when the distance and time separating pairs of sources is less than the space and time thresholds chosen by the user, and the space threshold is relaxed with distance from the center of the network to account for the decreased accuracy in the LMA with distance. Both Murphy (2006) and Bruning and MacGorman (2013) conducted a sensitivity study on the space and time thresholds. Murphy (2006) found that flash counts were most stable when the space and time thresholds exceeded 5 km and 0.2 s, respectively, and that flash counts increased rapidly for

TABLE 2. Details of the times and locations of VHF sources used for the flash counting case study and the resulting flash counts by method for each storm mode.

	Storm mode		
	Single cell	MCS	Supercell
Date	4 Jul 2010	14 Jun 2011	20 May 2011
Time (UTC)	1900–1928	2350–2351	1000–1001:20
Area (km^2)	80 × 80	60 × 60	140 × 140
Latitude range (°)	35.1–35.8	34.9–35.5	34.9–36.25
Longitude range (°)	−98.3 to −97.4	−98.05 to −97.35	−98.6 to −97.0
Manual count	101	87	98
Algorithm—150 ms	111	111	90
Algorithm—200 ms	108	98	87
Algorithm—250 ms	107	90	87

smaller values. Bruning and MacGorman (2013), using data from two supercell thunderstorms, found that the spatial threshold is most stable between 1 and 6 km and deduced that for consistency with other studies, it is best to use a 3-km spatial threshold and a 0.15-s temporal threshold.

Because Bruning and MacGorman (2013) used only data from supercell thunderstorms in their study, whereas a climatology will consist of lightning from all different storm modes, a small case study was conducted to test how the temporal criterion changes depending on storm mode. Three different storm types were chosen: a single-cell thunderstorm from 4 July 2010, a supercell thunderstorm from 14 June 2011, and a mesoscale convective system (MCS) from 20 May 2011. Table 2 summarizes the times and areas evaluated for each storm mode. Flash counts were determined first with a subjective manual count. Because identifying and counting flashes by hand is time intensive, a small time period and area were chosen such that approximately 100 flashes were identified by hand for each storm mode. After the manual counts were complete, the algorithm was run on the same LMA data using a spatial threshold of 3 km and temporal thresholds of 0.15, 0.20, and 0.25 s. Neither the manual count nor any of the algorithm flash counts are considered more or less correct; rather, the most stable solution for all storm modes is considered the best option for the temporal threshold.

Table 2 shows a summary of the flash counts for each method for each storm mode. Note that the number of flashes counted by each of the three algorithms was more than the number counted manually for the single-cell and MCS cases but was less than the number of flashes counted for the supercell case. This result suggests that higher flash rates and a higher frequency of small flashes found in supercell storms as compared to other storm modes (e.g., Bruning and MacGorman 2013; Calhoun et al. 2013; Schultz et al. 2015; Bruning and Thomas 2015) make it hard for the algorithm to detect all of the flashes in supercell storms, even directly over the network, where flash detection efficiency is calculated to be 99% (Chmielewski and Bruning 2016).

With these observations in mind, the algorithm was run using a spatial threshold of 3 km and a temporal threshold of 0.25 s. The flashes were then used to create a plot of flash extent density, which is a count of the number of times lightning flashes propagate through each grid cell in a horizontal two-dimensional grid. Flashes for the Junes 2007–11 dataset have been sorted, and the resulting summation of flash extent densities on a 10 km × 10 km grid are shown in Fig. 3c.

4. Method comparison and summary

As can be seen by comparing Fig. 3b to Fig. 3c, both the normalization method and the flash-sorting method yield a similar result over large time scales. The biggest differences occur at ranges larger than 125 km, where there are no sources removed by the normalization method and where the flash detection efficiency is smallest (Chmielewski and Bruning 2016). For further comparison of the two methods, shorter time scales (days and months) were also examined. Three months were chosen—a winter month (January 2007), a spring month (May 2011), and a summer month (August 2009) (Fig. 4). Similarly, three days with three different storm modes were chosen—20 June 2007 (MCS), 10 May 2010 (supercells), and 25 July 2011 (single cells) (Fig. 5). Because neither method is absolutely correct, the comparisons merely look for similarities and differences between the two methods to determine any patterns in coverage that may make one method advantageous over the other, depending on its application.

The differences between the two techniques are similar for both the monthly and daily time scales. Source density plots created using the normalization method and flash extent density plots created using the flash-sorting method for monthlong time scales (January 2007,

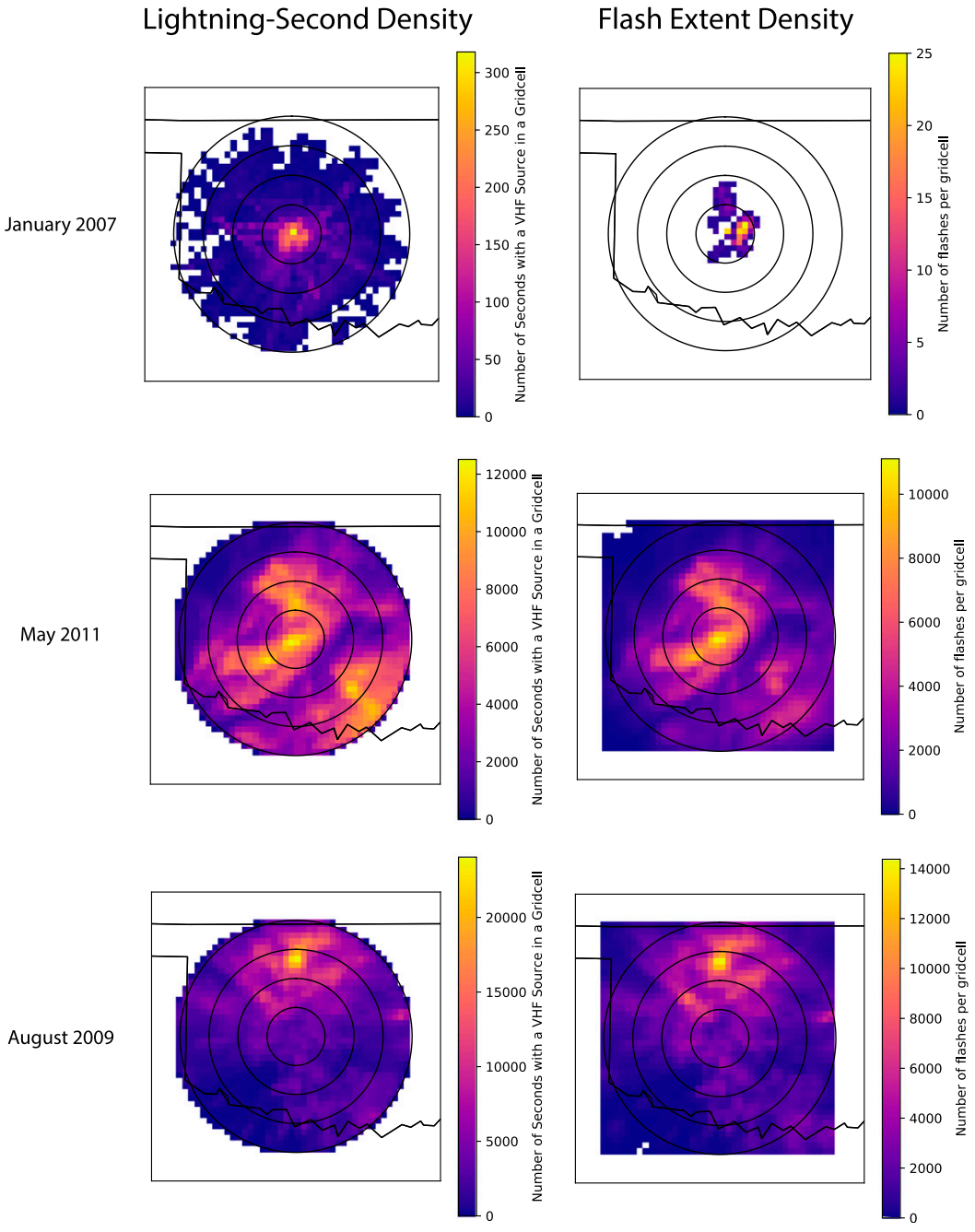

FIG. 4. Lightning-second densities from (left) normalized data and (right) flash extent densities for January 2007, May 2011, and August 2009. For each plot, the black rings mark distance every 50 km from the center of the OKLMA and densities increase from purple to yellow on the color scale.

May 2011, and August 2009) are shown in Fig. 4. The two methods yield a similar result, with two notable exceptions. The first difference is seen in the data from January 2007, where the normalization method leaves a much broader extent of lightning activity over the network than the flash-sorting method. Some of what the flash-sorting method has removed is recognizable as radiation from aircraft flying through ice clouds (e.g., Thomas et al. 2004). The radiation from aircraft can be seen as straight lines of sources in the January 2007 source density plot in Fig. 4. The radiation from aircraft and from other nonlightning noise are absent from the flash extent density plot because the VHF sources did not cluster to meet the

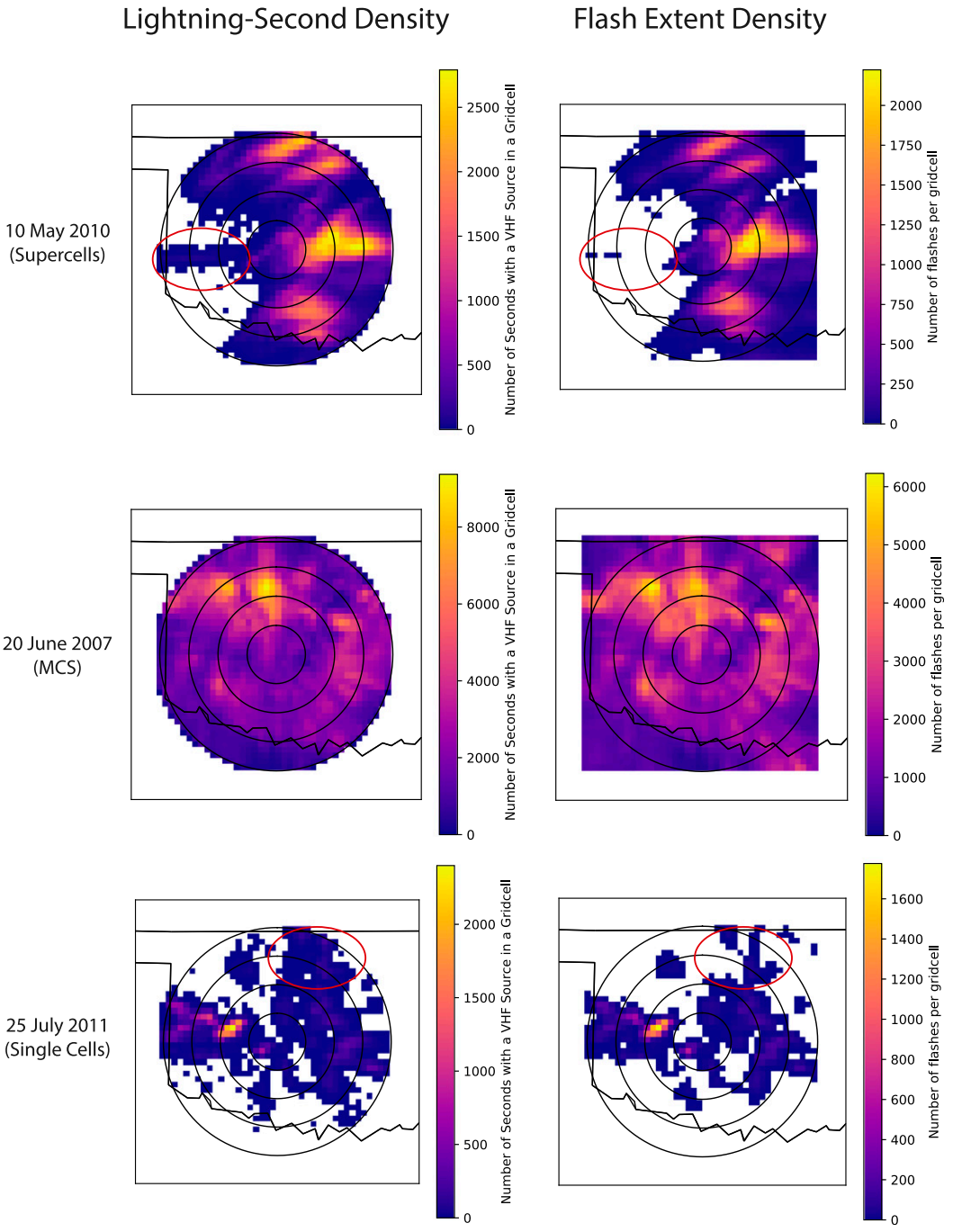

FIG. 5. As in Fig. 4, but for individual days rather than months. Supercells were the dominate storm mode on 10 May 2010, a mesoscale convective complex was dominate on 20 Jun 2007, and single cells were prevalent on 25 Jul 2011. The red ellipse on the 10 May 2010 and 25 Jul 2011 plots highlights where the normalization method indicates lightning activity that is not categorized as flashes by the flash-sorting algorithm.

10-source minimum required by the flash-sorting method. It is unclear whether the rest of the VHF sources included by the normalization method but not the flash-sorting method is caused by noise or lightning. The second major difference in methods can be seen in the May 2011 plots, as the flash-sorting method indicates more flashes directly over the network than in southeastern Oklahoma, while the source density plot shows a more equal distribution of radiation sources across the domain.

Source density and flash extent density plots for individual days are shown in Fig. 5. Again, with the daily plots there are slight variations in the location of maxima of lightning activity, but the overall pattern of coverage is the same for both methods with two exceptions. On 10 May 2010 there is an east–west line of VHF sources caused by noise that is seen in the lightning-second density plot but that has been filtered out by the flash-sorting method. The day with the least amount of data, 25 July 2011, also had a noticeable difference in results between the two methods. The normalization method indicates there was lightning in the northeastern portion of the domain, while the flash-sorting method has less coverage of lightning flashes in that region (red circles in plots).

Both the flash-sorting and normalization methods work to alleviate the problem of detection efficiency being higher directly over the network than farther away from the network. The same general patterns in lightning activity are present no matter which method is used; however, the normalization method removes more sources directly over the LMA than the flash-sorting method removes flashes, which can cause discrepancies where there are maxima in lightning activity. The flash-sorting method is especially good at weeding out noise (e.g., airplane tracks), but it may be missing smaller individual flashes at the farther ranges of the network, as seen in the 25 July 2011 example and possibly the January 2007 example, which may be problematic for case studies of wintertime thunderstorms or for days with single-cell thunderstorms. The flash size criteria or flash algorithm criteria may need to be tweaked to improve results in those cases, as in Fuchs et al. (2015), who changed the flash size criteria depending on the sensitivity of the LMA being used. Overall, it is recommended that the flash-sorting algorithm be used for future studies of large sets of LMA data because of its skill in eliminating extraneous sources and for consistency between networks and case studies, but understanding that it may have limitations in cases where there are relatively few flashes.

Acknowledgments. The authors thank the three anonymous peer reviewers of this manuscript, whose comments made us think more deeply about the results presented and improved the overall quality of this work. Thank you to Doug Kennedy and Dennis Nealson, who helped install stations and who maintained operation of the Oklahoma Lightning Mapping Array (OKLMA). The authors also acknowledge Paul Krehbiel, Bill Rison, Ron Thomas, Harald Edens, and others on their team at New Mexico Tech, who developed the Lightning Mapping Array and provided technical assistance for system operation and data processing. This research and the OKLMA were supported in part by Office of Naval Research Grant N00014-00-1-0525, and by NOAA NESDIS Grants NA11OAR4320072 and NA16OAR4320115; NSF Grant 1063945; NOAA/Office of Oceanic and Atmospheric Research under NOAA–University of Oklahoma Cooperative Agreement NA11OAR4320072, U.S. Department of Commerce; and NASA Grant NNX16AD24G.

REFERENCES

Bruning, E. C., and D. R. MacGorman, 2013: Theory and observations of controls on lightning flash size spectra. *J. Atmos. Sci.*, **70**, 4012–4029, https://doi.org/10.1175/JAS-D-12-0289.1.

——, and R. J. Thomas, 2015: Lightning channel length and flash energy determined from moments of the flash area distribution. *J. Geophys. Res. Atmos.*, **120**, 8925–8940, https://doi.org/10.1002/2015JD023766.

Calhoun, K. M., D. R. MacGorman, C. L. Ziegler, and M. I. Biggerstaff, 2013: Evolution of lightning activity and storm charge relative to dual-Doppler analysis of a high-precipitation supercell storm. *Mon. Wea. Rev.*, **141**, 2199–2223, https://doi.org/10.1175/MWR-D-12-00258.1.

Chmielewski, V. C., and E. C. Bruning, 2016: Lightning Mapping Array flash detection performance with variable receiver thresholds. *J. Geophys. Res. Atmos.*, **121**, 8600–8614, https://doi.org/10.1002/2016JD025159.

Chronis, T., L. D. Carey, C. J. Schultz, E. V. Schultz, K. M. Calhoun, and S. J. Goodman, 2015: Exploring lightning jump characteristics. *Wea. Forecasting*, **30**, 23–37, https://doi.org/10.1175/WAF-D-14-00064.1.

Darden, C. B., D. J. Nadler, B. C. Carcione, R. J. Blakeslee, G. T. Stano, and D. E. Buechler, 2010: Utilizing total lightning information to diagnose convective trends. *Bull. Amer. Meteor. Soc.*, **91**, 167–175, https://doi.org/10.1175/2009BAMS2808.1.

Fuchs, B. R., and Coauthors, 2015: Environmental controls on storm intensity and charge structure in multiple regions of the continental United States. *J. Geophys. Res. Atmos.*, **120**, 6575–6596, https://doi.org/10.1002/2015JD023271.

Hamlin, T., 2004: The New Mexico Tech lightning mapping array. Ph.D. dissertation, New Mexico Institute of Mining and Technology, 164 pp.

Koshak, W., and Coauthors, 2004: North Alabama Lightning Mapping Array (LMA): VHF source retrieval algorithm and error analyses. *J. Atmos. Oceanic Technol.*, **21**, 543–558, https://doi.org/10.1175/1520-0426(2004)021<0543:NALMAL>2.0.CO;2.

Kuhlman, K. M., C. L. Ziegler, E. R. Mansell, D. R. MacGorman, and J. M. Straka, 2006: Numerically simulated electrification and lightning of the 29 June 2000 STEPS supercell storm. *Mon. Wea. Rev.*, **134**, 2734–2757, https://doi.org/10.1175/MWR3217.1.

MacGorman, D. R., and Coauthors, 2008: TELEX: The Thunderstorm Electrification and Lightning Experiment. *Bull. Amer. Meteor. Soc.*, **89**, 997–1013, https://doi.org/10.1175/2007BAMS2352.1.

McCaul, E., S. J. Goodman, K. LaCasse, and D. Cecil, 2009: Forecasting lightning threat using cloud-resolving model simulations. *Wea. Forecasting*, **24**, 709–729, https://doi.org/10.1175/2008WAF2222152.1.

Murphy, M., 2006: When flash algorithms go bad. *Proc. First Int. Lightning Meteorology Conf.*, Tucson, AZ, Vaisala, 6 pp., https://my.vaisala.net/en/events/ildcilmc/Documents/When%20Flash%20Algorithms%20Go%20Bad.pdf.

Rison, W., R. J. Thomas, P. R. Krehbiel, T. Hamlin, and J. Harlin, 1999: A GPS-based three-dimensional lightning mapping system: Initial observations in central New Mexico. *Geophys. Res. Lett.*, **26**, 3573–3576, https://doi.org/10.1029/1999GL010856.

Schultz, C. J., W. A. Petersen, and L. D. Carey, 2009: Preliminary development and evaluation of lightning jump algorithms for the real-time detection of severe weather. *J. Appl. Meteor. Climatol.*, **48**, 2543–2563, https://doi.org/10.1175/2009JAMC2237.1.

——, L. D. Carey, E. V. Schultz, and R. J. Blakeslee, 2015: Insight into the kinematic and microphysical processes that control lightning jumps. *Wea. Forecasting*, **30**, 1591–1621, https://doi.org/10.1175/WAF-D-14-00147.1.

Thomas, R. J., P. R. Krehbiel, W. Rison, S. Hunyady, W. P. Winn, T. Hamlin, and J. Harlin, 2004: Accuracy of the Lightning Mapping Array. *J. Geophys. Res.*, **109**, D14207, https://doi.org/10.1029/2004JD004549.